MODELING CARDIAC CELL BIOPHYSICS USING DEEP LONG-SHORT MEMORY NETWORKS

Bruna Gonçalves

Graduate Student
Norfolk State University
700 Park Avenue
Norfolk, VA, USA
b.s.goncalves@spartans.nsu.edu

Makarand Deo

Department of Engineering
Norfolk State University
700 Park Avenue
Norfolk, VA, USA
mdeo@nsu.edu

ABSTRACT

Human induced pluripotent stem cell-derived cardiomyocytes (hiPSC-CMs) are being used to investigate mechanisms of various life-threatening cardiac disorders and drug effects. The Long Short-Term Memory (LSTM) is a type of neural networks that have become popular for finding patterns from the previous time steps to help predict the future response. In this paper, we developed a Deep LSTM (DLSTM), to represent the electrophysiological response of a typical hiPSC-CM. Our model is able to reproduce experimentally observed effects on the action potential (AP) morphology for alterations in 5 main ionic currents in hiPSC-CMs. The DLSTM model achieved an impressive accuracy of 98.5% when compared to a detailed mathematical model of hiPSC-CM based on AP duration parameters (APD_{50}, APD_{75}, APD_{90}). The proposed approach has the potential to reduce the computational time of multiscale cardiac electrophysiology simulations and can be used in mechanistic studies to investigate inherited arrhythmia syndromes and patient-specific drug therapies.

Keywords: Deep Learning, stem cell-derived cardiomyocytes, cardiac electrophysiology modeling.

1 INTRODUCTION

Engineering strategies to use steam cells in biological research is one of the breakthrough biological discoveries of the 21th century. Stem cells have a remarkable potential to differentiate into many cell types, and with recent advances in cell differentiation techniques, they may provide viable alternative to specific human cell types such as nerve cells, kidney cells, cardiac myocytes etc. Human Induced Pluripotent Stem Cells (hiPSCs) is a class of stem cells derived from specialized somatic cells that have been reprogrammed to become pluripotent. hiPSC-derived cardiomyocytes (hiPSC-CMs) have recently been used successfully in studying cardiac safety pharmacology and various inherited as well as acquired cardiac arrhythmia disorders (Moretti et al., 2010). The Comprehensive *in vitro* Proarrhythmia Assay (CiPA) initiative stipulates research directions around the use of hiPSC-CM experimental data and mathematical modeling in proarrhythmic risk assessment (Colatsky et al., 2016).

Accurate numerical biophysical models can be employed to elucidate mechanisms of cardiac rhythm disorders and their clinical implications. The predictive modeling has been increasingly used to investigate the missing link between experimental observations and clinical translation. Recently, Akwaboah et al. (Akwaboah et al., 2021) formulated a detailed model of hiPSC-CMs which is able to accurately reproduce the biophysical dynamics of hiPSC-CMs. The model consists of ionic current formulations of 14 key channels, pumps and exchangers along with intracellular calcium homeostasis. The model was used to provide insights into the causes of the experimentally observed suppression of automaticity in hiPSC-CMs during cholinergic stimulation.

The movement of various ions, such as sodium (Na^+), potassium (K^+) and Calcium (Ca^{2+}), across the cell membrane through voltage gated channels gives rise to changes in transmembrane voltage, called action potential (AP). A typical AP of cardiac myocyte consists of five phases. 1) Phase 0, a resting phase, where the membrane potential is almost steady in the range of -60mV to -80mV. Inward rectifier potassium current, I_{K1} and pacemaker current, $I_{f,}$ play major roles in this phase. 2) Phase 1, rapid depolarization phase resulting from fast sodium current (I_{Na}) occurring at suprathreshold voltage conditions. 3) Phase 2, a brief repolarization resulting from transient outward potassium currents (I_{to}). 4) Phase 3, a plateau formed from a contention between inward L-type calcium current (I_{CaL}) and ultra-rapid delayed rectifier potassium current (I_{kur}). 5) Phase 4, a rapid repolarization phase dominated mostly by rapid delayed rectifier potassium current (I_{kr}). Figure 1 shows a typical AP of hiPSC-CM and key currents responsible in each phase.

From modeling perspective, the AP is a process that needs information from the past and present states to predict the future behavior, known as a time series. In recent decades, deep Artificial Neural Networks (ANNs) have captured the world's attention by offering novel solutions to complex modeling of time series. Recurrent Neural Networks (RNNs) and Long Short-Term Memory (LSTM) are classes of neural networks that have gained popularity in handling time series data (Han et al., 2021; Weerakody et al., 2021). RNNs contain gates which are activated at each time step, allowing information to be stored for the next time step in order to provide a temporal memory property. However, these gates are not capable of storing long-term information. To resolve this problem, Hochreiter and Schmidhuber (Hochreiter & Schmidhuber, 1997) developed the LSTM algorithm as a modification to RNN (Pascanu et al., 2013) that is able to retain valuable information for long term, which is essential for non-linear times series prediction (Peter & Matskevichus, 2019).

In this study, we propose a deep LSTM (DLSTM) model for predicting the AP of an hiPSC-CM. A DLSTM consists of multiple cascaded LSTM layers operating at different time scales (Pascanu et al., 2014). This method can perform an ordered process for capturing data patterns in a complex temporal task. We utilized two different DLSTM architectures to compare the performance of AP time series prediction.

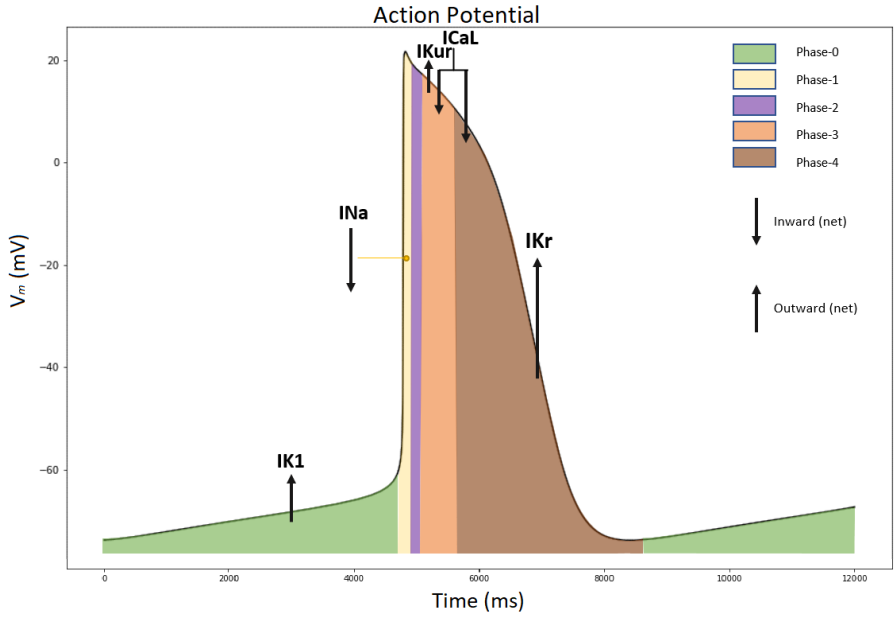

Figure 1. A typical action potential of an hiPSC-CM showing various phases of the action potential and main ionic currents active during each phase.

2 METHODS

2.1 LSTM Model

The LSTM model developed by Hochreiter et al. (Hochreiter & Schmidhuber, 1997) solved the vanishing gradient problem of RNNs that improved the long-term memory of the network. In our design, the AP time series information is stored in more than 1000 discrete time steps using a cell state (memory cell). The cell state runs for an entire time step and works as a bridge with the ability to add or remove information in the cell state, carefully managed by structures called gates. There are 3 different gates in an LSTM cell (see Figure 2): forget gate (f_t), input gate (i_t), and output gate (o_t). The output of an LSTM cell is the hidden state (h_t) which is used as an additional input for the next cell.

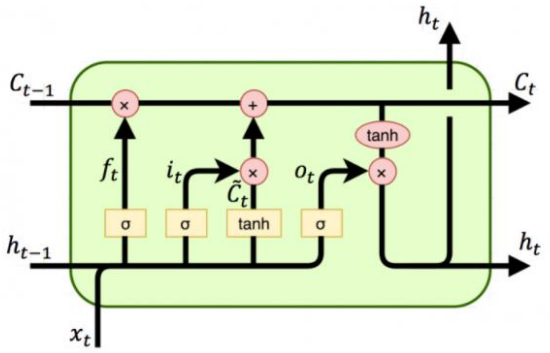

Figure 2: The LSTM bock diagram [9].

The forget gate has a sigmoid activation function (σ) which passes information from the current input (x_t) and the prior hidden state (h_{t-1}) as given below. When the output value is close to 0, it implies forget, and when it is close to 1, it signifies keep.

$$f_t = \sigma\,(W_f \cdot [h_{t-1}, x_t] + b_f) \tag{1}$$

where *t* is timestep, W_f is a weight matrix of the forget gate, current input (x_t) and the prior hidden state (h_{t-1}) and b_f is the connection bias as t.

In the input gate, a second sigmoid function also receives the current state (x_t) and the previously hidden state (h_{t-1}). The values are changed from 0 (not important) to 1 (important). Next, the x_t and h_{t-1}will pass to a tanh operator and create a vector ($\check{\mathrm{C}}_t$) with values between -1 and 1. The output values for sigmoid and tanh functions are suitable for point-by-point multiplication as shown below.

$$i_t = \sigma\,(W_i \cdot [h_{t-1}, x_t] + b_i) \tag{2}$$

$$\check{\mathrm{C}}_t = \tanh\,(W_c \cdot [h_{t-1}, x_t] + b_c) \tag{3}$$

Where b_i is the bias vector, $\check{\mathrm{C}}_t$ is the value generated by tanh, W_c is the weight matrix of tanh, and b_c is bias vector at t.

The cell state is generated by two steps. First, through the multiplication between the previous cell state (C_{t-1}), and the forget vector. If the result is 0, the values in the cell state will be discarded. Next, the network runs point-by-point addition on the output value of the input vector (i_t), giving the network a new cell state (C_t). In the last step, the output gate determines the value of the next hidden state. A third sigmoid function receives the current state (x_t) and the previously hidden state (h_{t-1}). The new cell state (C_t) passes through a tanh function. These two values are then multiplied point-by-point. The network selects which information the hidden state should store based on the final value. Prediction is based on this hidden state.

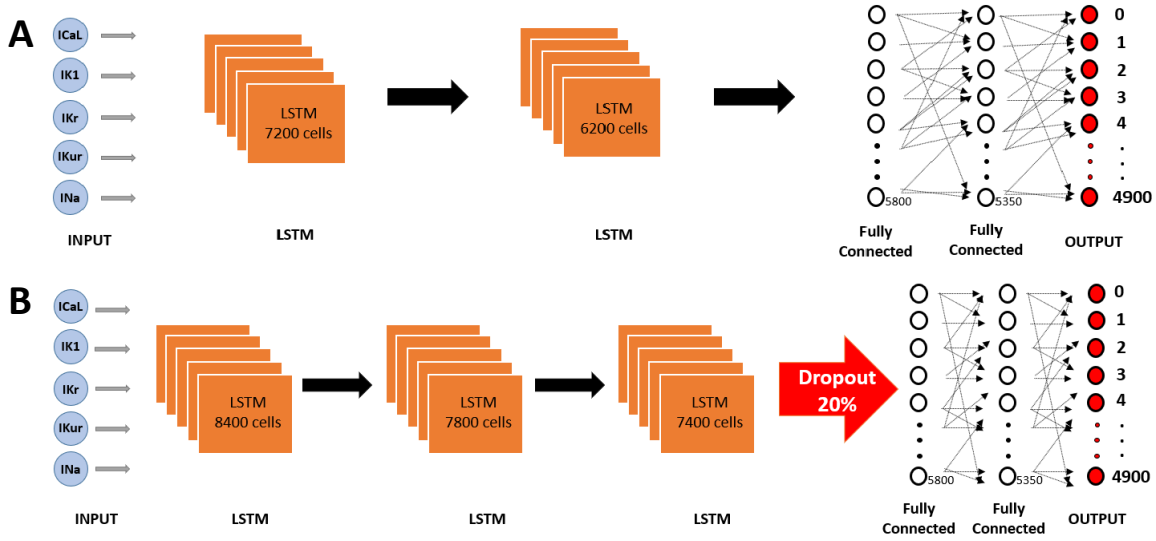

Figure 3: The proposed network designs for hiPSC-CM model. A) DLSTM2, and B) DLSTM3.

$$o_t = \sigma\left(W_o \cdot [h_{t-1}, x_t] + b_{o)}\right) \tag{4}$$

$$h_t = O_t * tanh\left(C_t\right) \tag{5}$$

Where h_t is the next hidden value, and (C_t) the next value for the cell state. Finally, the new cell state and hidden state are then passed forward to the next time step.

2.2 The Proposed Network Architectures

Our deep neural network architecture uses a combination of LSTM layers, dropout (to decrease overfitting), and fully connected dense layers. To achieve the most effective network, we implemented two different architectures. The first architecture, shown in Figure 3A, used two back-to-back LSTM layers followed by three fully-connected dense layers. This network will be referred to as DLSTM2. The second architecture, shown in Figure 3B, composed of three back-to-back LSTM layers, one dropout, and three fully-connected dense layers. This network will be referred to as DLSTM3.

For the training, we chose Mean Square Error (MSE) loss function and Adam optimizer for adaptive learning rate (Goodfellow et al., 2016). The batch size was chosen to be 12. The data was randomly divided into 80% for training and the remaining 20% for testing. Scaling factors for the maximum conductance of five main ion currents: I_{Na}, I_{Kur}, I_{Kr}, I_{K1} and I_{CaL}, were used as inputs to both the networks.

2.3 Generation of Data

Training and testing data was created by simulating the original Akwaboah et al. model (Akwaboah et al., 2021). The maximum channel conductance values of I_{Na}, I_{Kur}, I_{Kr}, I_{K1} and I_{CaL} currents were scaled in the range of 0% (complete block) to 200% (100% enhancement) in steps of 20%. Each simulation was run for a duration of 5000 ms with a time step of 0.05 ms, generating a total of 100,000 points. This strategy gave us a total of 321 scenarios. However, we invalidated some of the data for not producing an AP due to non-physiological values of the current conductance. As a result, our final data set consisted of 252 samples with 100,000 time points each. To facilitate analysis, we selected four samples of 12000 output points each, capturing a complete AP signal in each sample as shown in Figure 4. Next, we downscaled the data using a Fourier method in SciPy library to transform the samples into 5000 points each. Lastly, we deleted the first 50 and last 50 points due to susceptibility of noise.

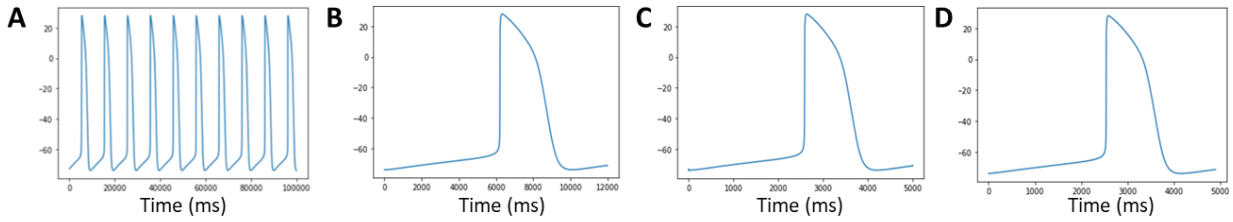

Figure 4: Downsampling of AP data. A) Original AP time series containing 100,000 time points. B) One of the 4 split AP data. C) The AP data after the downsampling. D)Final data sample with 4900 time points.

2.4 Postprocessing and Performance Metric

Our goal was to create a DLSTM capable of replicating the shape of an AP, automaticity and the values of AP durations at 50%, 75% and 90% of the maximum amplitude (APD_{50}, APD_{75}, APD_{90}, respectively) using only the values of the current conductance scaling.

To counteract noise in the DLSTM output, we applied a Gaussian filter for 1-dimension using SciPy library.

$$g_\sigma(x) = \frac{1}{\sqrt{2\pi}\sigma} \exp\left(-\frac{x^2}{2\sigma^2}\right) \tag{6}$$

Where σ is the standard deviation.

As mentioned before, we selected the Mean Square Error metric to penalize the weights which is computed by:

$$MSE = \frac{1}{n} \sum_{i=1}^{n} |y_i - \hat{y}_i| \tag{7}$$

Where y is the observed values, ŷ is the predicted values and n the number of data points.

To compare our results with the experimental data we used mean absolute percentage error (MAPE) which is calculated by:

$$MAPE = \frac{100}{n} \sum \left|\frac{y - \hat{y}}{y}\right| \tag{8}$$

Where y is the observed values, ŷ is the predicted values and n the number of data points.

3 RESULTS AND DISCUSSION

We trained the DLSTM2 model for 923 epochs and DLSTM3 model for 1175 epochs. Each epoch was completed in an average 2.5 minutes and 6 minutes for DLSTM2 and DLSTM3 models, respectively, using a CPU environment. Table I lists the two-performance metrics MSE, and MAPE for the outcome of models when compared with the Akwaboah et al. model (Akwaboah et al., 2021). MSE represents the overall accuracy of the model output, while the MAPE measures the difference between the predicted and actual values of APD_{50}, APD_{75}, APD_{90} and APD_{all}. The Gaussian σ values for smoothing out the predicted signal were varied between 1 to 7 in steps of 0.1. The best value of σ was found to be 2.2 for DLSTM2 and 2.1 for DLSTM3 model. Higher σ values produced distortions in the steep AP regions such as the upstroke (Phase 1-2) and maximum AP amplitude. It is evident from Table 1 that the DLSTM3 model exhibits a better accuracy than the DSLTM2 model. It was expected that the DSLTM3 model had a better prediction than the DLSTM2 because as we increase the depth of the model, it gains the ability to learn more complex temporal data patterns. In fact, both models were able to reliably produce AP morphologies of hiPSC-CMs with loss values closer to 0.

Table 1: Performance Comparison of the AP Models.

Model	APD_{50} (MAPE)	APD_{75} (MAPE)	APD_{90} (MAPE)	APD_{all} (MAPE)	Loss Evaluate for the model (MSE)
DLSTM2 $\sigma = 2.2$	2.331%	1.91%	2.268%	2.17%	0.086
DLSTM3 $\sigma = 2.1$	1.356%	1.166%	1.175%	1.232%	0.068

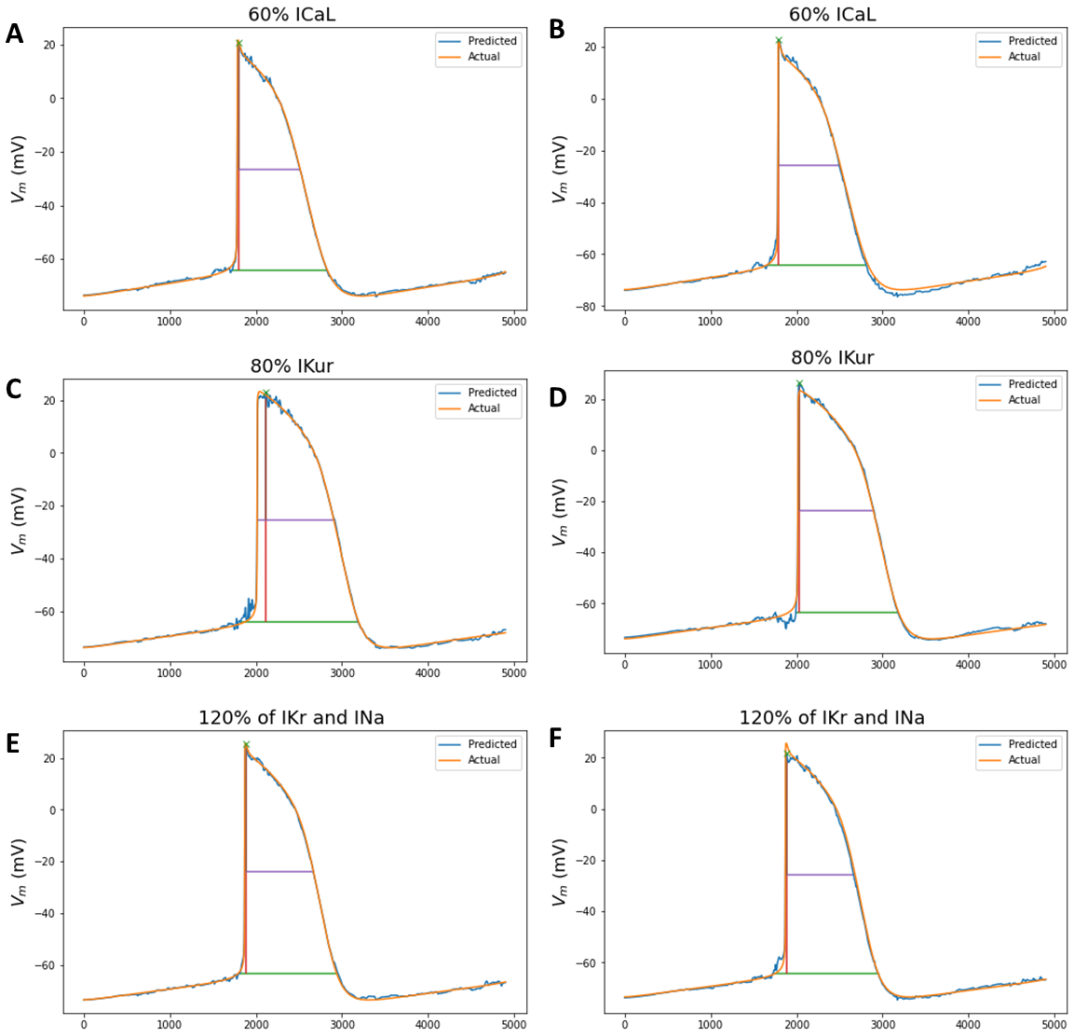

Figure 5: Sample AP traces produced by DLSTM2 (left column) and DLSTM3 (right column) models overlayed with true traces from Akwaboah model for various combinations of current conductance. The APD_{50} and APD_{90} measurements are shown in the AP traces.

Figure 5 shows representative examples of the AP produced by the DLSTM models for various scaling of ionic currents. The predictions of DLSTM3 model were smoother than the DLSTM2 model. However, in both models some noise was observed during AP plateau (Phase 2-3) and diastolic interval (Phase 0) despite Gaussian smoothing.

More importantly, the models were able to reproduce the experimentally observed behavior in cardiac myocytes (Ma et al., 2011) such as: 1) prolongation of AP when I_{Kr} or I_{Kur} are blocked and shortening of

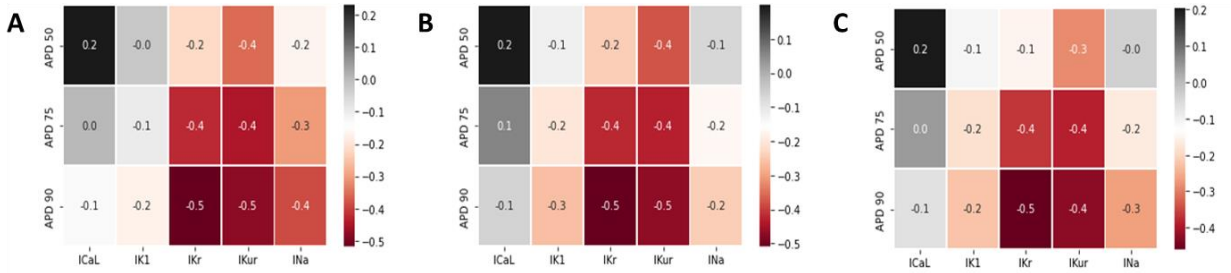

Figure 6: Sensitivity analysis in A) original Akwaboah, B) DLSTM2 and C) DLSTM3 models to study the effects of variations in I_{Na}, I_{Kur}, I_{Kr}, I_{K1} and I_{CaL} on the APD parameters.

AP when I_{Kr} or I_{Kur} are enhanced, 2) shortening of AP plateau when I_{CaL} was blocked and prolongation when I_{CaL} was enhanced, 3) depolarization of maximum diastolic potential when $I_{K1}$was blocked and hyperpolarization when I_{K1} was enhanced. Figure 6 shows a detailed comparative sensitivity analysis of the DLSTM models (Panels B and C) and that of the original Akwaboah model (Panel A) for the five main ionic currents and their effects on APD parameters. The figure shows color-coded correlation coefficients corresponding to the relation between the currents and AP durations. The figure shows a strong positive correlation coefficient between APD_{50} and I_{CaL}, which indicates that an increase in I_{CaL} causes an increase in APD_{50}. I_{Kr} and I_{Kur}, on the other hand, show a strong negative correlation with APD_{90} and APD_{75}. I_{K1} shows an almost neutral correlation with APD. These results demonstrate that our DLSTM models can faithfully produce the biophysical effects of ionic channel variations just as good as the detailed models. These analyses are important because they show that our models can be utilized to study the effects of various anti-arrhythmia drugs (Paci et al., 2020) such as E4031 and Dofetilide (potassium channel blockers), Diltiazem and Verapamil (calcium channel blockers), and flecainide (sodium channel blocker). Our models are also useful in studying arrhythmia mechanisms in inherited cardiomyopathies such as long/short QT syndrome (SQTS/ LQTS), catecholaminergic polymorphic ventricular tachycardia (CPVT) and Brugada syndrome (Vaidyanathan et al., 2016). This study demonstrates the feasibility and effectiveness of AI-based biophysical models as an alternative to traditional ODE solvers, thereby drastically reducing the amount of computations and simulation time of multiscale simulations.

4 CONCLUSION

Over the years, the applications for deep learning have increased exponentially, and time series is no exception. The LSTM's ability to find and keep patterns over many time steps is crucial for applications in non-linear time series, and the success of recent implementations have proven its importance. In this study, deep LSTM-based models were developed to describe the biophysical response of human induced pluripotent stem cell-derived cardiomyocytes. The models were trained with data from alterations in five main ionic current components that contribute to the action potentials in these cells. The model with 3 cascaded LSTM layers achieved an overall MSE of 0.068 and the action potential morphology was reproduced with accuracy closer to 99%. These models were able to faithfully reproduce experimentally observed behaviors of ion channel blocks and drug interactions in cardiomyocytes. Further study should involve creating further finetuned models with the capacity to manipulate more currents, stimulus conditions, and refractory periods.

REFERENCS

Akwaboah, A. D., Tsevi, B., Yamlome, P., Treat, J. A., Brucal-Hallare, M., Cordeiro, J. M., & Deo, M. (2021). An in silico hiPSC-Derived Cardiomyocyte Model Built With Genetic Algorithm. *Frontiers in Physiology*, *12*. https://doi.org/10.3389/fphys.2021.675867

Colatsky, T., Fermini, B., Gintant, G., Pierson, J. B., Sager, P., Sekino, Y., Strauss, D. G., & Stockbridge, N. (2016). The Comprehensive in Vitro Proarrhythmia Assay (CiPA) initiative — Update on progress. *Journal of Pharmacological and Toxicological Methods*, *81*, 15–20. https://doi.org/10.1016/j.vascn.2016.06.002

Goodfellow, I., Bengio, Y., & Courville, A. (2016). *Deep Learning*. MIT Press.

Han, Z., Zhao, J., Leung, H., Ma, K. F., & Wang, W. (2021). A Review of Deep Learning Models for Time Series Prediction. In *IEEE Sensors Journal* (Vol. 21, Issue 6). https://doi.org/10.1109/JSEN.2019.2923982

Hochreiter, S., & Schmidhuber, J. (1997). Long Short-Term Memory. *Neural Computation*, *9*(8). https://doi.org/10.1162/neco.1997.9.8.1735

Ma, J., Guo, L., Fiene, S. J., Anson, B. D., Thomson, J. A., Kamp, T. J., Kolaja, K. L., Swanson, B. J., & January, C. T. (2011). High purity human-induced pluripotent stem cell-derived cardiomyocytes: Electrophysiological properties of action potentials and ionic currents. *American Journal of Physiology - Heart and Circulatory Physiology*, *301*(5), 2006–2017. https://doi.org/10.1152/ajpheart.00694.2011

Moretti, A., Bellin, M., Welling, A., Jung, C. B., Lam, J. T., Bott-Flügel, L., Dorn, T., Goedel, A., Höhnke, C., Hofmann, F., & others. (2010). Patient-specific induced pluripotent stem-cell models for long-QT syndrome. *New England Journal of Medicine*, *363*(15), 1397–1409.

Paci, M., Passini, E., Klimas, A., Severi, S., Hyttinen, J., Rodriguez, B., & Entcheva, E. (2020). All-Optical Electrophysiology Refines Populations of In Silico Human iPSC-CMs for Drug Evaluation. *Biophysical Journal*, *118*(10), 2596–2611. https://doi.org/10.1016/j.bpj.2020.03.018

Pascanu, R., Gulcehre, C., Cho, K., & Bengio, Y. (2014). How to construct deep recurrent neural networks. *2nd International Conference on Learning Representations, ICLR 2014 - Conference Track Proceedings*.

Pascanu, R., Mikolov, T., & Bengio, Y. (2013). On the difficulty of training recurrent neural networks. *30th International Conference on Machine Learning, ICML 2013, PART 3*.

Peter, G., & Matskevichus, M. (2019). Hyperparameters Tuning for Machine Learning Models for Time Series Forecasting. *2019 6th International Conference on Social Networks Analysis, Management and Security, SNAMS 2019*. https://doi.org/10.1109/SNAMS.2019.8931860

Vaidyanathan, R., Markandeya, Y. S., Kamp, T. J., Makielski, J. C., January, C. T., & Eckhardt, L. L. (2016). IK1-enhanced human-induced pluripotent stem cell-derived cardiomyocytes: An improved cardiomyocyte model to investigate inherited arrhythmia syndromes. *American Journal of Physiology - Heart and Circulatory Physiology*, *310*(11), H1611–H1621. https://doi.org/10.1152/ajpheart.00481.2015

Weerakody, P. B., Wong, K. W., Wang, G., & Ela, W. (2021). A review of irregular time series data handling with gated recurrent neural networks. *Neurocomputing*, *441*. https://doi.org/10.1016/j.neucom.2021.02.046

AUTHOR BIOGRAPHIES

BRUNA SILVEIRA GONCALVES is a Graduate Research Assistant at Norfolk State University. She is currently enrolled in the Master of Science in Electronics Engineering program. She holds a Bachelor of Science in Electronics and Electrical Engineering. Her research interests lie simulation modeling, especially in healthcare. Her email address is b.s.goncalves98@gmail.com.

MAKARAND DEO is an Associate Professor in the Department of Engineering at Norfolk State University, Norfolk, VA. His research interests include multiscale modeling and simulation of cardiac electrophysiology and biosensing systems. His email address is mdeo@nsu.edu.